

Low-Temperature, Mercury-Mediated Synthesis of Aluminum Intermetallics

Mikhail Khoudiakov and Arthur B. Ellis*

Department of Chemistry, University of Wisconsin—Madison, 1101 University Avenue,
Madison, Wisconsin 53706

John H. Perepezko* and Sungtae Kim

Department of Materials Science and Engineering, University of Wisconsin—Madison,
1509 University Avenue, Madison, Wisconsin 53706

Keith D. Kepler

PolyStor, 6940 Sierra Court, Dublin, California 94568

Received January 12, 2000. Revised Manuscript Received May 4, 2000

The preparative-scale synthesis of intermetallic phases in the Al–Au and Al–Pd systems can be achieved at the relatively low temperature of boiling Hg (~350 °C at 1 atm). In particular, Al₂Au, AlAu, AlAu₂, Al₃Pd₂, and AlPd can be made in high yield either as single products or as multiple products by dissolution of the elements in liquid Hg, followed by distillation of the solvent. The reaction products were determined by X-ray diffraction and electron microprobe analysis. A systematic study reveals that the products of these reactions depend strongly on initial mole ratios. A thermodynamic phase stability analysis was conducted using estimated free energies for the intermetallic phases. From these calculations and from the observed products and their sequence of formation, some of the reactions are shown to be kinetically controlled. Direct synthesis reactions tend to be favored for concentration ratios that correspond to intermetallic phases that exhibit a coexistence tie line with the Hg solution.

Introduction

Mercury is well known to form amalgams with most elements of the periodic table. The solubilizing ability exhibited by Hg allows it to be used as a flux for the low-temperature synthesis of intermetallics.¹ One of the earliest proposals for the use of mercury as a solvent appeared in 1930.² Since then, many binary and ternary systems have been studied extensively, particularly by electrochemical techniques.³ However, in most cases the product phases were not isolated from the amalgams. There are only a few reports where this method was used as a preparative technique, and none of them, to our knowledge, has defined the scope and limitations of this synthetic methodology. To date, the method has been used to prepare several Al–Ni phases,⁴ Fe–Zn phases,⁵ InSb crystals,⁶ Pt–Cu, Pt–Zn, Pt–Sn, Pt–In, and Pt–Al intermetallics,⁷ and various alloys of rare-earth elements (Y, Sm, Gd, Dy, Ho, and Er) with transition metals (Mn, Fe, Co, Ni, Cu, Ag, and Au).⁸ There is also a recent report describing epitaxial growth

of CdTe from a mercury solvent that leads to films of very good quality and crystallinity.⁹ The aforementioned intermetallics highlight a significant advantage of the mercury-mediated synthesis: instead of requiring high temperatures that in some cases exceed 1000 °C, liquid mercury (boiling point ~350 °C at 1 atm) provides a milder preparative route that may also afford the opportunity to access kinetically-controlled products that represent a decrease in the overall free energy but not absolute minima. This permits isolation of metastable phases that cannot be readily obtained at higher temperatures.

In this paper we report the successful extension of this synthetic methodology to the preparation of the Al₂Au, AlAu, AlAu₂, Al₃Pd₂, and AlPd intermetallics. All of these intermetallics were prepared in high yield either as single products or as multiple products by dissolving the elements in liquid Hg, followed by distillation of the solvent. Previously, all of these intermetallics required temperatures in the range of 650–1650 °C for their synthesis directly from the elements. We also show through a systematic study that the products of these reactions depend strongly on initial mole ratios. A thermodynamic phase stability analysis is used to demonstrate that some of the reactions are kinetically controlled, based on the observed products and their

(1) Elwell, D. *Crystal Growth from High-Temperature Solutions*; Academic Press: London, 1975.

(2) Russel, A. S. *Nature* **1930**, *125*, 89.

(3) Galus, Z. *CRC Crit. Rev. Anal. Chem.* **1975**, *359*.

(4) Fitzer, E.; Gerasimoff, P. Z. *Metallkd.* **1959**, *50*, 87.

(5) Lihl, F.; Demel, A. Z. *Metallkd.* **1952**, *43*, 307.

(6) Faust, J. W.; Johh, H. F. *J. Phys. Chem. Solids* **1964**, *25*, 1407.

(7) Barlow, M.; Planting, P. J. Z. *Metallkd.* **1969**, *60*, 292.

(8) Kirchmayr, H. R. Z. *Metallkd.* **1965**, *56*, 767.

(9) Sangha, S. P. S.; Medland, J. D.; Berry, J. A.; Rinn, I. M. J. *Cryst. Growth* **1987**, *83*, 127.

sequence of formation. Direct synthesis reactions tend to be favored for concentration ratios that correspond to intermetallic phases that exhibit a coexistence tie line with the Hg solution.

Experimental Section

Aluminum powder (325 mesh, 99.97%), palladium powder (325 mesh, 99.99%), and gold splatters (99.999%) were obtained from Cerac; nickel powder (325 mesh, 99.9%) was obtained from Johnson Matthey Co. Mercury (99.99%) was obtained from Aldrich and purified after each use by first filtering through a No.2 Whatman filter and then washing in 10% nitric acid, followed by rinsing with distilled water. The mercury solutions of metals were made by placing measured amounts of metal powders into a 100-mL round-bottomed flask and then pouring in the mercury on top of the powder. The combined atomic ratio of the metal components to the mercury was about 0.5–2 atom % (typically ~1 g of the metal mixture/~50 mL of Hg), which was generally sufficient to completely dissolve the reactant metals at ~350 °C (the boiling point of mercury at 1 atm is 357 °C). The flask was connected to a distillation apparatus that was kept under house nitrogen (dried over calcium sulfate) and heated in a sand bath for about 10–24 h. The mercury then was distilled under vacuum at 200–250 °C to isolate the product. Resulting intermetallics were characterized by X-ray powder diffraction using a Scintag PAD V diffractometer (Cu K α radiation) and by elemental analysis using inductively coupled plasma (ICP) emission spectroscopy on a Leeman Labs Inc. ICP 2.5 instrument. The samples for ICP analyses were prepared by dissolving the powder in concentrated HCl, HNO₃, or aqua regia and then diluting the solution into the ppm range with distilled water. Standard solutions of pure elements were prepared in the same fashion. A Cameca SX50 instrument was used for electron microprobe analysis (EMPA) and wavelength dispersive spectroscopy (WDS) with the voltage set to optimize the analysis of small particles. Oxide and metal standards were used for calibration.

Warning! Hazards associated with mercury are well known. All manipulations with this material should be performed with care and in a well-ventilated safety hood. Vacuum distillation of mercury is potentially a very dangerous procedure. We recommend testing all new flasks for defects prior to conducting the synthesis by heating them under vacuum at ~300 °C. Specialized high-temperature grease like Apiezon AP 100 or 101 should be used on the joint between the flask and the distillation head to prevent mercury vapor leaks. To decrease the thermal strain in the distillation column, we recommend cooling the condenser with air rather than water. It is absolutely necessary to install a removable trap cooled with liquid nitrogen between the outlet of the distillation apparatus and the oil pump. It is important to note that the intermetallic compounds obtained by this technique may contain traces of mercury even after prolonged heating under vacuum. For this reason the products should be stored in a tightly closed vial.

Table 1. Powder Diffraction and Elemental Analysis Data for Al–Au Intermetallics

initial ratio Al:Au ^a	product composition ^b	elemental analysis (Al:Au ratio) ^c
2:1	Al ₂ Au ^d	1.86 ± 0.09
1:1	AlAu, ^e Al ₂ Au, ^d AlAu ₂ , ^f and Au	1.12 ± 0.06 ^g
1:2	AlAu, ^e AlAu ₂ , ^f Au, and Al ₂ Au ^{d,h}	0.72 ± 0.04 ^g

^a Mole ratio of Al:Au dissolved in Hg prior to the reaction. ^b Products identified by X-ray powder diffraction. ^c ICP analysis of the product powder. ^d JCPDS 17-0877. ^e JCPDS 30-0019. ^f JCPDS 26-1005. ^g Metallic gold was physically removed prior to analysis. ^h Only in one out of four runs with Al:Au = 1:2 was Al₂Au observed and then only as a small amount.

Results

Intermetallics in the Al–Au System. The binary phase diagram of the Al–Au system is well established.¹⁰ There is still some debate concerning the 70–90 atom % Au region,¹¹ but the compounds Al₂Au, AlAu (three modifications), and AlAu₂ are well characterized. Using mercury as a solvent is ideal for Al, because there are no known Al–Hg intermediate phases.¹⁰ The solubility of Al in mercury is ~4 atom % at ~350 °C. The solubility of gold in mercury is ~35 atom % at ~350 °C. The Au–Hg system is more complex, and a number of intermediate phases are known.¹⁰ However, a control experiment demonstrated that Au–Hg intermetallics are not formed under the present experimental conditions: vacuum distillation of a 0.2 atom % solution of Au in Hg yields metallic gold with no detectable mercury contamination by ICP emission spectroscopy (less than 1 ppm). The observation of Au precipitation instead of the formation of one or more of the more stable Au–Hg intermediate phases is a clear example of a kinetically-controlled reaction.

Three different reactions with the initial Al:Au ratios of 2:1, 1:1, and 1:2 were investigated. The results are summarized in Table 1. A single-phase product was obtained for the Al:Au ratio of 2:1. This Al₂Au intermetallic phase is a dark purple solid that is sometimes observed on overheated circuit boards when the two metals are used in close proximity.¹² When Al and Au are mixed in the 1:1 ratio, the major product is AlAu, according to X-ray powder diffraction, but significant amounts of Al₂Au and AlAu₂ are also formed along with a small amount of metallic gold. This probably accounts for the slightly higher Al content observed in the final mixture for this ratio. When mercury is distilled from a solution of Al and Au in the 1:2 ratio, a mixture of AlAu, AlAu₂, and Au is generally obtained. However, one of four runs resulted in the formation of a small amount of Al₂Au along with AlAu, AlAu₂, and Au. This is another example of kinetic control, in which the product yield is sensitive to processing.

Electron microprobe studies were performed on the products obtained with the 2:1 and 1:1 Al:Au ratios. A backscattered electron image of Al₂Au particles obtained from the 2:1 Al:Au ratio experiment is shown in Figure 1a. The average particle size is about 5 μ m, but a

(10) Massalski, T. B. *Binary Alloy Phase Diagrams*; ASM International: Materials Park, OH, 1990.

(11) Hansen, M.; Andreko, K. *Constitution of Binary Alloys*; McGraw-Hill Book Co.: New York, 1958.

(12) Ellis, A. B.; Geselbracht, M. J.; Johnson, B. J.; Lisensky, G. C.; Robinson, W. R. *Teaching General Chemistry: A Materials Science Companion*; American Chemical Society: Washington, DC, 1993; p 119.

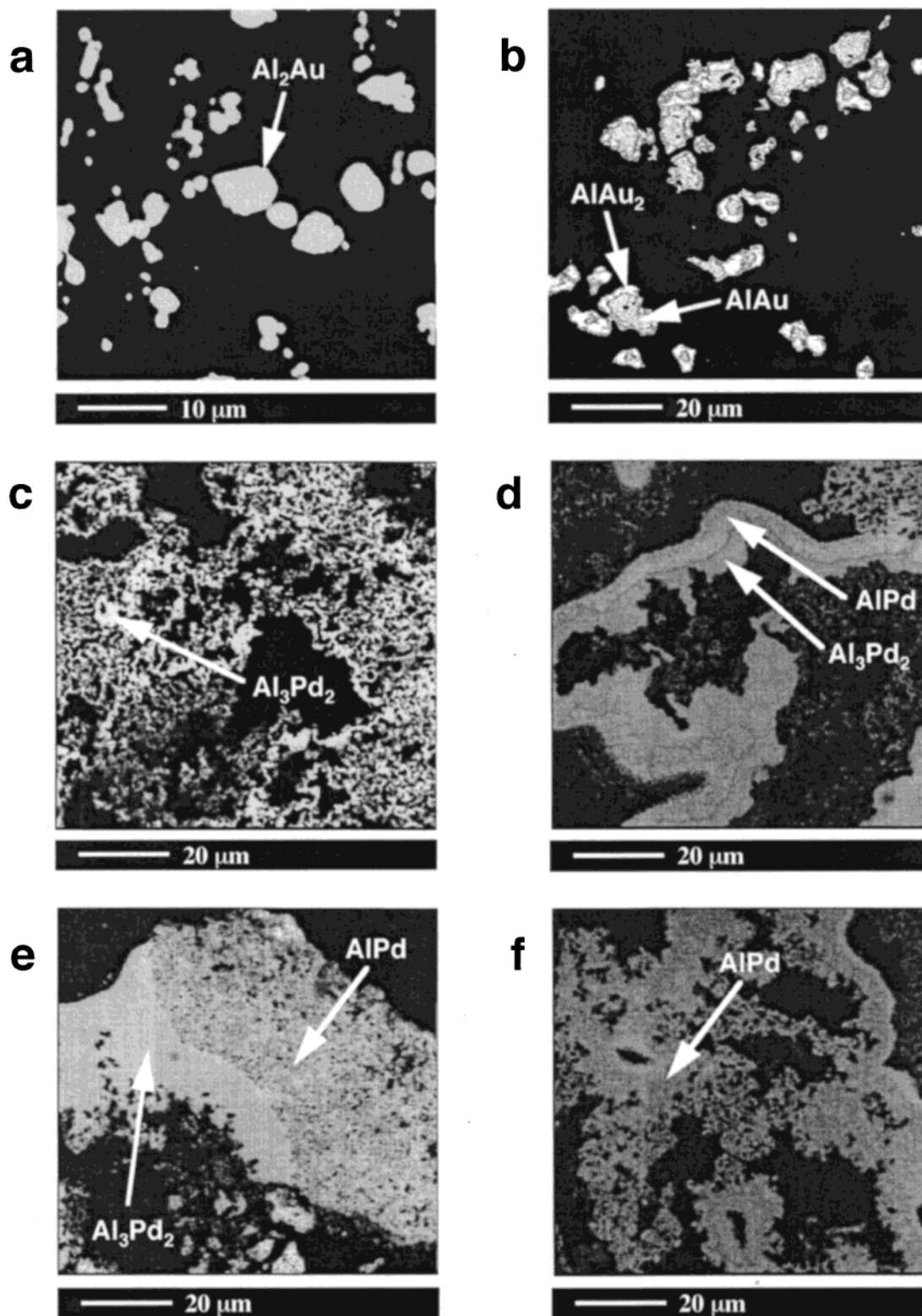


Figure 1. Backscattered electron images of Al–Au and Al–Pd intermetallics prepared by codissolving the elements in Hg, as described in the text, in the indicated mole ratios: (a) Al:Au = 2:1, (b) Al:Au = 1:1, (c) Al:Pd = 2:1, (d) Al:Pd = 3:2, (e) Al:Pd = 1:1 (one-step distillation), (f) Al:Pd = 1:1 (two-step distillation).

number of submicron particles are also present. A WDS analysis confirmed that Al_2Au is the only product. The average Al:Au ratio is 1.91 ± 0.10 , which is in good agreement with the elemental analysis data obtained from ICP emission spectroscopy.

Figure 1b shows a backscattered electron image of the powder obtained by the distillation of a 1:1 Al:Au

mercury solution. It is clear that, unlike the case for Al_2Au , the composition varies within the individual particles, with the interior being close to AlAu in composition and the shell being close to AlAu_2 . This is indicative of sequential formation of AlAu and AlAu_2 , whereas Al_2Au is presumably formed independently (see the Discussion section).

Table 2. Powder Diffraction and Elemental Analysis Data for Al–Pd Intermetallics

initial ratio Al:Pd ^a	product composition (X-ray) ^b	elemental analysis (Al:Pd ratio) ^c
2:1	Al ₃ Pd ₂ ^d and Al ^e	2.00 ± 0.10
3:2	Al ₃ Pd ₂ ^d and AlPd ^f	1.47 ± 0.07
1:1 ⁱ	Al ₃ Pd ₂ , ^d AlPd, ^f and (Pd) ^g	1.07 ± 0.05
1:1 ^j	AlPd ^f	1.12 ± 0.06
1:2	HgPd ^h and AlPd ^f	0.57 ± 0.03

^a Mole ratio of Al:Pd dissolved in Hg prior to the reaction. ^b Products identified by X-ray powder diffraction. ^c ICP analysis of the product powder. ^d JCPDS 06-0654. ^e JCPDS 04-0787. ^f JCPDS 29-0065. ^g Pd–Al solid solution. ^h JCPDS 13-0149. ⁱ One-step distillation (see text for details). ^j Two-step distillation (see text for details).

Intermetallics in the Al–Pd System. The six well-established compounds in the Al–Pd system are Al₄Pd, Al₂₁Pd₈, Al₃Pd₂, AlPd (high-temperature and two low-temperature modifications), Al₃Pd₅, and AlPd₂.¹⁰ The solubility of Pd in mercury is ~1 atom % at 350 °C. Palladium is known to interact strongly with mercury, as was confirmed by a control experiment: vacuum distillation of a 0.35 atom % solution of Pd yields a residue that was identified as HgPd by X-ray powder diffraction.

Four different compositions with the 2:1, 3:2, 1:1, and 1:2 Al:Pd ratios were investigated. The results are summarized in Table 2. The residue obtained from a solution of Al and Pd in the 3:2 ratio contains both Al₃Pd₂ and AlPd. Al₃Pd₂ also can be prepared in pure form. To achieve this, an excess of Al must be used (a 2:1 Al:Pd ratio was used in our case). Immediately after distillation, the residue contains highly reactive metallic aluminum, which can be easily separated by allowing it to react with ambient oxygen for about 1 h and then removing the thin fuzz of alumina that has formed with a gentle stream of air. Pure AlPd can be prepared by mixing Al and Pd in the 1:1 ratio. However, a special procedure has to be used: if the distillation of a starting solution is carried out in one step, i.e., until all of the mercury is removed, a mixture of Al₃Pd₂, AlPd, and metallic Pd or Pd–Al solid solution is obtained; if the distillation is stopped when approximately ³/₄ of the solvent is removed, the flask is cooled to room temperature and then reheated to complete the isolation, AlPd is found to be the major product based on X-ray diffraction data, another example of kinetically-controlled reactivity. An attempt to prepare the AlPd₂ intermetallic using a 1:2 Al:Pd ratio was unsuccessful. Even after 15 h of heating at ~350 °C in a vacuum, the product still contains a considerable amount of mercury. According to the powder diffraction data, the two major products are AlPd and HgPd.

Backscattered electron images of some Al–Pd intermetallic products obtained from these syntheses are shown in Figure 1c–f. EMPA data support the conclusion that Al₃Pd₂ (Figure 1c) and AlPd (Figure 1f) can be prepared in relatively pure form by this method. A WDS analysis of the powders containing more than one intermetallic product (Figure 1d,e) reveals that different Al–Pd phases do not form core–shell structures as in the case of the Al–Au system.

Intermetallics in the Al–Ni System. Although the synthesis of several Al–Ni intermetallics using mercury as a solvent was previously reported,⁴ all attempts to

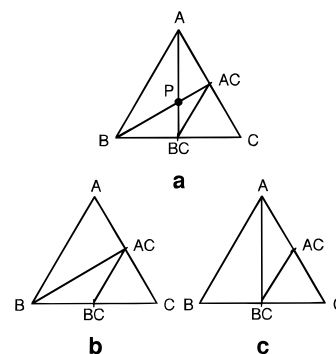


Figure 2. Schematic phase equilibria in a ternary system: (a) general case (as described in the text); (b) when $B + AC$ is more stable than $A + BC$; (c) when $A + BC$ is more stable than $B + AC$.

reproduce this work with the experimental setup described above were unsuccessful. Some indications of the formation of Al₃Ni₂, AlNi, and AlNi₃ were obtained, but the major components of the residue produced by distillation of the Al–Ni solutions were invariably metallic Ni for nickel-rich initial compositions, metallic Al for aluminum-rich ones, or a mixture of both for 1:1 ratio experiments. Apparently, the low solubility of Ni in mercury even at the boiling point (~0.01 atom %) prevents reaction from occurring. Products might be obtained either by increasing the temperature (the authors of the original report suggest a temperature range of 400–600 °C) or by using smaller amounts of starting materials. Because we were interested in preparative-scale yields of product under our experimental conditions, the study of the Al–Ni system was not pursued further.

Discussion

As noted earlier, there is a long history of the use of Hg as a solvent to form intermetallic phases by precipitation, but there has been little reported on the mechanisms of such reactions. An important initial step in developing an understanding of the operative mechanism is the identification of the reaction products corresponding to various initial reactant stoichiometries. The reaction products such as those identified in Tables 1 and 2 can be used to interpret the reaction pathway in terms of the relevant phase equilibria. This analysis also provides some insight into kinetic control of the reactions and their ability to yield metastable products by virtue of the low temperatures employed.

As a brief background to the analysis of synthetic reaction pathways, it is useful to recall some basic features in the analysis of multicomponent phase equilibria. For example, in an A–B–C ternary system (Figure 2a), five stable phases—A, B, C, AC, and BC—with line compositions are considered for analysis. The stable two-phase equilibrium lines on binary sides are A–B, A–AC, AC–C, BC–C, and B–BC. In the ternary region, there are three possible two-phase equilibrium lines: B–AC, A–BC, and AC–BC. Two-phase equilibrium lines for B–AC and A–BC are crossed at point P (Figure 2a). Comparing the free energies of B–AC and A–BC at point P allows for the identification of the

stable two-phase equilibrium line.^{13–15} The AC–BC line is stable, because no two-phase equilibrium line crosses over it. Therefore, establishing whether B–AC or A–BC is the stable two-phase equilibrium is essential in resolving the ternary system. At point P in Figure 2a, the equilibrium reaction becomes $A + BC \rightleftharpoons B + AC$. If the free energy change for reaction is negative, the products (B + AC) are thermodynamically stable (Figure 2b). If the free energy change is positive, the reactants (A + BC) are thermodynamically stable (Figure 2c). Therefore, estimating the free energy change for reaction $A + BC \rightleftharpoons B + AC$ identifies the more stable two-phase equilibrium line between the A–BC and B–AC lines.^{13–15} Of course, this simple illustration has ignored true ternary phases, but their presence does not change the basic method of analysis. Moreover, when certain binary phases are excluded from the synthesis reactions because of kinetic limitations, a similar approach can be applied to construct metastable phase diagrams.

The Al–Hg system does not contain any intermediate phases.^{16,17} In the Al–Hg system, Hg has a solubility range up to $X_{Al} = 0.04$. In the Au–Hg system, Hg has a solubility range up to $X_{Au} = 0.35$.¹⁷ The Au–Hg phase diagram shows the possible presence of intermediate phases, but for the conditions of the present experiments, there was no indication for the formation of any Au–Hg intermediate phases. Thus, the present estimation ignores the intermediate phases. In addition, the Al–Au phase diagram obtained from thin film studies shows five intermediate phases: Al_2Au , $AlAu$, $AlAu_2$, Al_2Au_5 , and $AlAu_4$.^{18,19} However, the existence of $AlAu_4$ at 350 °C is doubtful, and the thermodynamic model that we used shows that $AlAu_4$ is metastable. For the conditions of the present experiments, there was no evidence for the development of Al_2Au_5 or $AlAu_4$ phases. This excludes the $AlAu_4$ and Al_2Au_5 phases in estimating ternary phase equilibria. Based on the fact that none of the two-phase equilibrium lines in the Al–Au–Hg system cross one another, the ternary phase equilibria at 350 °C in terms of the relative phase stability are established (Figure 3) using the thermodynamically estimated data of phases (Table 3). In addition, it is important to stress that the phase equilibria presented in Figure 3 are metastable in character, because they reflect the observed kinetic difficulties in producing several of the phases reported in the companion binary equilibria.

In the case of the synthesis of Al–Au intermetallics, the resultant products indicate the phase equilibria that are illustrated in Figure 3 together with the initial reactant ratios. Under the kinetically-controlled conditions, the product phases observed with changing reactant ratios follow a relatively clear path, as noted in Figure 3. For example, with an initial Al: Au ratio of

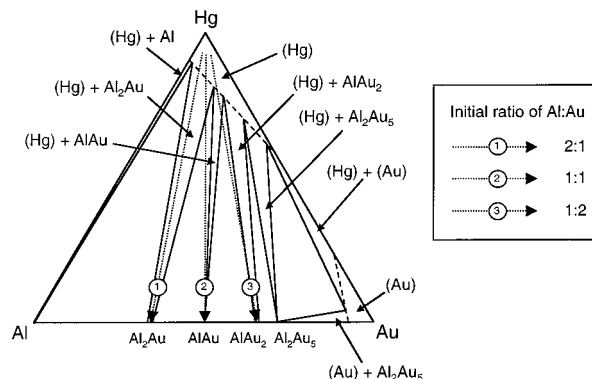


Figure 3. Schematic reaction paths for the evaluated phase equilibria of the Al–Au–Hg system at 350 °C (not to scale). Dotted lines reflect the changes in the average composition of the reaction mixture during the distillation. Estimated Hg-rich and Au-rich solution boundaries are shown as dashed lines.

Table 3. Calculated Free Energies of Formation of Phases in the Al–Au–Hg System at 350 °C

phase	thermodynamic model (kJ/mol) ^a	free energy at 350 °C (kJ/mol) ^b
Al_2Au	$-101.25 + 0.041T$	-62.0 ± 6.2
$AlAu$	$-85.128 + 0.045T$	-46.9 ± 4.7
$AlAu_2$	$-112.914 + 0.051T$	-64.0 ± 6.4
Al_2Au_5	$-245.546 + 0.110T$	-93.2 ± 9.3

^a Murray et al. constructed the phase diagram of the Al–Au system using the thermodynamic model described in ref 18; the calculated phase diagram is consistent with the experimental data.
^b Free energy calculated with respect to the standard states of Al(s), Au(s), and Hg(l) at 350 °C, using thermodynamic data in the Al–Hg, Al–Au, and Au–Hg systems.^{16–19}

2:1, the path (number 1) is directed toward precipitation of Al_2Au from the Hg solution. In addition, the Al_2Au phase with a phase field width representing deviations from stoichiometry in the binary system continues to be favored in the initial precipitation reaction as the composition ratio is varied to Au-rich values (see, for example, Table 1 for path number 2). This behavior can be represented in the isothermal section in Figure 3 by a series of three-phase regions relating the Al–Au intermetallic phases to the Hg solution phase. Moreover, the strong kinetic preference for precipitation of Al_2Au is apparent, because it is a product as the initial ratio varies from 2:1 to 1:1 and even to 1:2 (see below).

While the Al_2Au phase was attained as a single product for the initial ratio of 2:1, the mixed-phase products for initial ratios of 1:1 and 1:2 were often observed. As can be seen in Figure 3, the path (number 2) corresponding to the initial Al: Au ratio of 1:1 crosses the Al_2Au phase field, and this phase is, in fact, present in the product, as was shown by X-ray diffraction. As was noted earlier, an EMPA study of the product revealed a microstructure that indicates a sequential formation (Figure 1b). In fact, the $AlAu$ phase was observed to form with a surrounding shell of $AlAu_2$. Evidently, the presence of Al_2Au results in excess Au and leads to the development of $AlAu_2$.

For the initial Al: Au ratio of 1:2, the reaction path (number 3) crosses the $AlAu$ field and both $AlAu$ and $AlAu_2$ are observed products. One of the four syntheses with this ratio resulted in the formation of some amount of Al_2Au besides $AlAu$, $AlAu_2$, and Au. This again

(13) Kubaschewski, O.; Alcock, C. B.; Spencer, P. J. *Materials Thermochemistry*; Pergamon Press: New York, 1993.

(14) Gaskell, D. R. *Introduction to Metallurgical Thermodynamics*; McGraw-Hill Co.: New York, 1981.

(15) Lupis, C. H. P. *Chemical Thermodynamics of Materials*; Elsevier Science Publishing Co.: New York, 1983.

(16) McAlister, A. J. *Bull. Alloy Phase Diagrams* **1985**, *6*, 219.

(17) Okamoto, H.; Massalski, T. B. *Bull. Alloy Phase Diagrams* **1989**, *10*, 50.

(18) Murray, J. L.; Okamoto, H.; Massalski, T. B. *Bull. Alloy Phase Diagrams* **1987**, *8*, 20.

(19) Vandenberg, J. M.; Hamm, R. A. *J. Vac. Sci. Technol.* **1981**, *19*, 84.

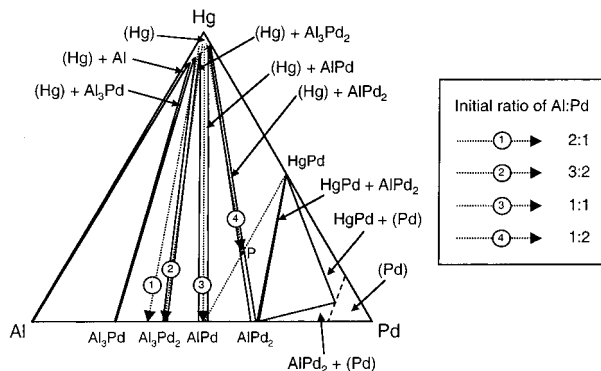


Figure 4. Schematic reaction paths for the evaluated phase equilibria of the Al–Pd–Hg system at 350 °C (not to scale). Dotted lines reflect the changes in the average composition of the reaction mixture during the distillation. Estimated Hg-rich and Pd-rich solution phase boundaries are shown as dashed lines.

suggests that the formation of Al_2Au is indeed very kinetically favored and at the same time implies that the reaction path for this ratio lies very near the Al_2Au phase field, because a very small change in the initial stoichiometry may lead to the formation of this phase.

In the Pd–Hg system, there is one intermediate phase HgPd and Hg has a solubility range up to $X_{\text{Pd}} = 0.01$.²⁰ In the Al–Pd system, four intermediate phases are stable at 350 °C and Pd has a solubility range up to $X_{\text{Al}} = 0.20$.^{21,22} This solid solution, then, has a two-phase equilibrium with HgPd. The free energy of the Pd solid solution is taken at $X_{\text{Al}} = 0.15$ in the Al–Pd system. The ternary phase equilibria and relative phase stability in the Al–Pd–Hg system at 350 °C are established (Figure 4) using the thermodynamically estimated data of phases (Table 4). The AlPd–HgPd two-phase line crosses over the Hg–AlPd₂ line. The free energy change of the equilibrium reaction $\text{AlPd} + \text{HgPd} \rightleftharpoons \text{Hg} + \text{AlPd}_2$ at point P in Figure 4 (–16 kJ/mol) indicates that the Hg–AlPd₂ two-phase equilibrium line is more stable than that for AlPd–HgPd. In this case, the AlPd–HgPd two-phase equilibrium line becomes metastable and is shown as a dotted line in Figure 4.

In the synthesis of Al–Pd intermetallics, the observed phase selection was also kinetically constrained so that only two of the several binary Al–Pd intermetallics developed during the synthesis reactions. For initial ratios of 2:1, 3:2, and 1:1 and the final elemental analysis ratios, the observed products are consistent with the metastable isothermal ternary phase diagram section given in Figure 4. It is not completely clear why a single product is not obtained for the initial ratio of 1:1, as one would expect from examining the phase

Table 4. Calculated Free Energies of Formation of Phases in the Al–Pd–Hg System at 350 °C

phase	mole fraction	free energy at 350 °C (kJ/mol) ^a
Al_3Pd	$X_{\text{Pd}} = 0.25$ (in Al–Pd)	-180 ± 9^b
Al_3Pd_2	$X_{\text{Pd}} = 0.42$ (in Al–Pd)	-348 ± 17^b
AlPd	$X_{\text{Pd}} = 0.50$ (in Al–Pd)	-156 ± 8^b
AlPd_2	$X_{\text{Pd}} = 0.67$ (in Al–Pd)	-202 ± 10^b
(Pd) ^c	$X_{\text{Pd}} = 0.85$ (in Al–Pd)	-29.9 ± 1.5^b
HgPd	$X_{\text{Pd}} = 0.50$ (in Hg–Pd)	-30.5 ± 3.4^d

^a Free energy calculated with respect to the standard states of Al(s), Pd(s), and Hg(l) at 350 °C, using thermodynamic data in the Al–Hg, Al–Pd, and Pd–Hg systems.^{16,20–22} ^b From activity data of Al evaluated by Ettenberg et al., activities of Pd at 1200 °C in the Al–Pd system were calculated;²² the entropy was estimated under the assumption that the heat of formation is independent of temperature, and using a temperature independent entropy, the free energies of formation at 350 °C were obtained.²³ ^c Pd–Al solid solution. ^d The enthalpy and entropy were assumed to be independent of temperature.²⁰

diagram. Most probably, the formation of AlPd, although thermodynamically favored, is kinetically constrained for this ratio and a two-step process is needed to accomplish it. For the Pd-rich ratio of 1:2, the AlPd₂ phase is not observed either separately or in association with AlPd because of the formation of HgPd. This signifies a changing phase stability and the development of an AlPd–HgPd–Hg three-phase field that effectively blocks Pd-rich intermetallics from coexisting with and precipitating from the Hg solution. In addition, this alternate phase equilibrium arrangement also reveals a key phase diagram feature in the design of intermetallic phase synthesis reactions based upon precipitation from Hg solutions: direct synthesis reactions are favored for intermetallic phases that exhibit a coexistence tie line with the Hg solution.

Conclusion

Mercury-assisted synthesis has been shown to be a practical method for making some binary intermetallics, provided that both metals are reasonably soluble in mercury at its boiling point. The preparation is impaired if one or both reactants interact strongly with mercury, although this difficulty can be overcome in some cases. For the two systems that were investigated in detail, there is a strong correlation between the binary phase diagram and the composition of the products isolated from mercury.

Acknowledgment. The authors thank Dr. John Fournelle for help with the Electron Microprobe studies and Greg Matzke for help with the synthesis. The work was supported by National Science Foundation Materials Research Science and Engineering Center (M.K. and A.B.E.) and the Army Research Office (DAAG55-97-1-0261 to J.H.P. and S.K.).

CM0000245

(20) Guminski, C. *Bull. Alloy Phase Diagrams* **1990**, *11*, 22.

(21) McAlister, A. J. *Bull. Alloy Phase Diagrams* **1986**, *7*, 368.

(22) Ettenberg, M.; Komarek, K. L.; Miller, E. *Metall. Trans.* **1971**, *2*, 1173.

(23) Ferro, R.; Capelli, R. *Mater. Nat.* **1963**, *34*, 659.